50

A HYBRID EXPLICIT-IMPLICIT HIGH-RESOLUTION METHOD FOR NON-LINEAR ADVECTION EQUATION

Igor MEN'SHOV, Munetsugu KANEKO, and Yoshiaki NAKAMURA
Department of Aerospace Engineering,
Nagoya University, Nagoya, 464-8603, Japan
Tel. 81-52-789-3394,3395
E-mail: menshov@nuae.nagoya-u.ac.jp, kaneko@aero4.nuae.nagoya-u.ac.jp,
nakamura@nuae.nagoya-u.ac.jp

A hybrid explicit/implicit numerical referred to as the CCG scheme was recently proposed by Collins, Collela, and Glaz for one-dimensional hyperbolic conservation laws. By suitable blending of an explicit second-order time marching scheme with an implicit scheme, this approach was made to possess the max norm diminishing (MND) property for all Courant numbers. Having been manifested for linear equations, the CCG scheme, however, fails to maintain this property unconditionally for non-linear equations, so that it requires an additional CFL-like restriction on the time step. In this paper we show how to remedy the shortcoming of the CCG scheme, and also propose a new general approach to design unconditionally MND hybrid schemes for non-linear advection equations. Numerical experiments are carried out for calculating the Burgers equation on a highly non-uniform grid. Results of these calculations exhibit a certain advantage in accuracy and efficiency of the proposed hybrid scheme compared with both the conventional implicit and the second-order explicit schemes.

1 Introduction

The present paper is concerned with an important problem of computing unsteady fluid flows with small scale features such as boundary layer, shock wave, contact discontinuity, shear layer, which are characterized by steep gradients in their spatial distributions. To handle this problem, solution adaptive grids are being commonly used. These grids consist of fine meshes to accurately resolve those steep gradients in the solution along with rather coarse meshes in moderate gradient zones. Such non-uniformity in mesh spacing is characterized by the grid stiffness defined as the ratio of the smallest grid mesh spacing to the largest.

The method presented in this paper is mostly intended for unsteady solutions on highly stiff grids. The grid stiffness is commonly accompanied by the temporal stiffness, when explicit schemes are used to perform time integration. Because of the CFL stability condition, the time step must be proportional to the smallest mesh spacing. Therefore, a deadlock situation might occur, where local refinement of the grid makes explicit schemes impractical to use due to almost vanishing time step.

On the other hand, implicit methods are mostly unconditionally stable, and the choice of the step size for time marching calculations is dictated by required temporal accuracy only. However, there is a shortcoming that all of these methods suffer from excessive numerical diffusion, which is much larger than that of explicit methods. Accordingly, it is ineffective to use implicit schemes for unsteady problems. Therefore, the problem is to design an accurate numerical method that could stably calculate unsteady problems with a relatively large time step not restricted by the grid stiffness.

Regarding the above problem, in this paper we propose a hybrid scheme which includes both implicit and explicit schemes. It has an advantage of high efficiency inherent in implicit schemes and high accuracy inherent in explicit schemes.

The idea of implicit-explicit hybridization has been explored by several researchers. First, it was discussed in the book of Richtmyer and Morton[1]. Collins *et.al.*[2] developed a hybrid scheme referred to as the CCG scheme for one dimensional Eulerian hydrodynamics. O'Rourke *et.al.*[3] extended the CCG scheme to multidimensional advection calculations.

The design principles of the CCG scheme are as follows.

1. Continuous switching between implicit and explicit schemes.
2. Second-order of accuracy in the explicit mode.
3. Max Norm Diminishing Property (MND) for all time steps.

The CCG scheme has been first designed for the one-dimensional linear advection equation

$$\partial_t u + a\partial_x u = 0 \tag{1}$$

where a is a positive constant. In this scheme eq.(1) is discretized by the finite volume method (FVM),

$$u_i^{n+1} = u_i^n - \lambda(u_{i+1/2} - u_{i-1/2}) \tag{2}$$

where $\lambda = a\Delta t/\Delta x_i$.

The edge state $u_{i+1/2}$ is defined depending on the CFL number λ as follows:

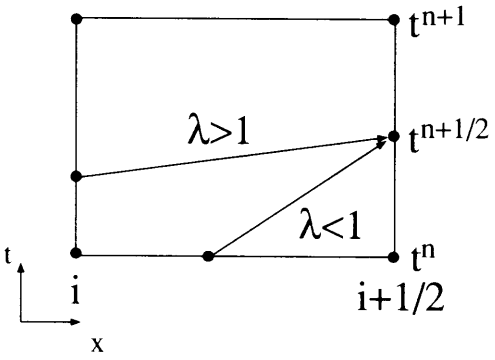

Figure 1: Interpolation scheme of CCG.

$$u_{i+1/2} = \begin{cases} u_i^n + 0.5(1-\lambda)\delta u_i^n & \lambda \leq 1 \\ \frac{1}{\lambda} u_i^n + \frac{1-\lambda}{\lambda} u_i^{n+1} & \lambda > 1 \end{cases} \quad (3)$$

where δu_i^n is a limited difference defined in such a way that there exist coefficients $c_i^{\pm}$ to satisfy

$$\delta u_i^n = c_i^+ \Delta u_{i+1/2} = c_i^- \Delta u_{i-1/2},\ 0 \leq c_i^{\pm} < +\infty \quad (4)$$

The baseline idea of the CCG is to use different intervals of interpolation for calculating the edge state. The choice of the interpolation interval is decided based on the location of the characteristic line, as shown in Fig.1.

Then, the CCG scheme was extended to a non-linear equation[2]

$$\partial_t u + \partial_x [f(u)] = 0 \quad (5)$$

where $f' > 0$ and $f'' > 0$

This equation is discretized as

$$u_i^{n+1} = u_i^n - \frac{\Delta t}{\Delta x_i} [f(u_{i+1/2}) - f(u_{i-1/2})] \quad (6)$$

and the edge state is calculated as

$$u_{i+1/2} = \begin{cases} u_i^n + 0.5(1-\lambda_i)\delta u_i^n & \lambda_i \leq 1 \\ \frac{1}{\lambda_i} u_i^n + \frac{1-\lambda_i}{\lambda_i} u_i^{n+1} & \lambda_i > 1 \end{cases} \quad (7)$$

where $\lambda_i = a_i \Delta t / \Delta x_i, and\ a_i = f'(u_i^n)$.

All the above design principles are clearly manifested for the linear equation. However, in the non-linear case, eqs. (6) and (7) fail to maintain the MND property for all time steps, and may produce incorrect numerical solutions. One example of this is shown in Fig. 2, where the CCG scheme is applied to solve eq. (5) with $f(u) = 0.5u^2$ and initial data in the form of a triangle on a non-uniform grid with a stiffness ratio of 0.01. The computational intervals are also depicted in Fig. 2. It is seen that an erroneous peak appears just behind the shock in the region of fine meshes. A remedy against this phenomenon has been proposed in [2], which is in fact a restriction on the time step similar to the CFL condition. This circumstance almost cancels the advantages originally declared for the CCG scheme.

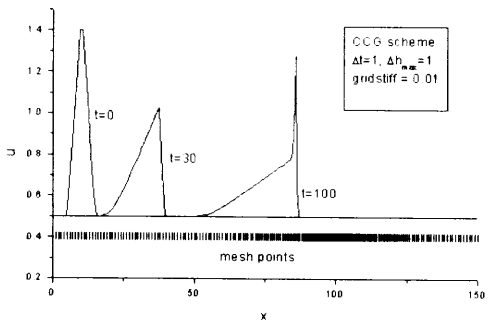

Figure 2: Shortcoming of the CCG scheme.

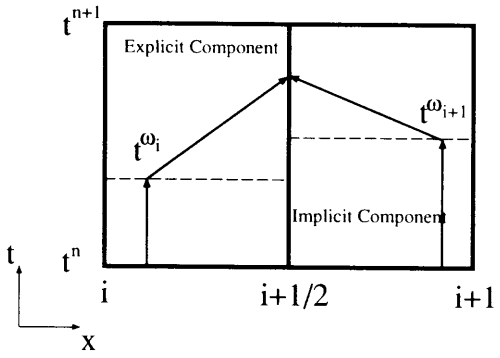

Figure 3: Geometrical interpretation to the hybrid scheme.

The aim of the present paper is to overcome the above problem of the CCG scheme and develop a new accurate hybrid scheme that would make the CCG design principles valid even for non-linear equations. The development of this scheme is carried out under the following conditions:

1. It must maintain the MND property for all time steps.
2. Its explicit constituent must be maximally enforced.

Our strategy is as follows:

1. develop a baseline hybrid scheme that would have unconditionally the MND property for non-linear equations.
2. apply a FCT(Flux Correctored Transport) technique[4] to enforce the explicit constituent.

2 Baseline Hybrid MND Scheme

2.1 One-dimensional scalar equation

We start with the case of a scalar conservation law

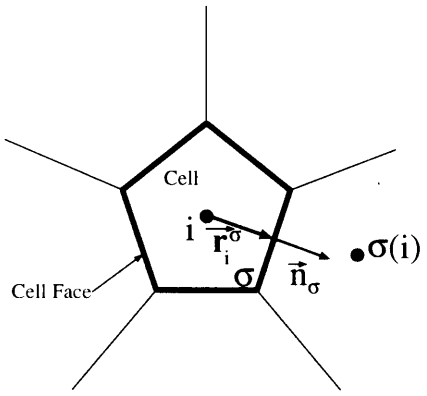

Figure 4: Sketch for multi-dimensional discretization.

$$\partial_t u + \partial_x [f(u)] = 0 \tag{8}$$

where $f'' > 0$ and $a = f'(u)$.

This is discretized by the FVM as:

$$u_i^{n+1} = u_i^n - \frac{\Delta t}{\Delta x_i} \left[F_{i+1/2} - F_{i-1/2} \right] \tag{9}$$

where $F_{i+1/2}$ is a numerical flux function associated with the cell interface and considered as a function of $u^l_{i+1/2}$ and $u^r_{i+1/2}$, the values of u on the left- and right-hand sides of the interface, respectively.

$$F_{i+1/2} = F(u^l_{i+1/2}, u^r_{i+1/2}) \tag{10}$$

There is a variety of choices for this numerical flux. We use a relatively simple HLL(Harten-Lax-Leer)[5] approximation method:

$$F(u_1, u_2) = \frac{s^+_{1/2} f_1 - s^-_{1/2} f_2 + s^+_{1/2} s^-_{1/2} (u_2 - u_1)}{s^+_{1/2} - s^-_{1/2}} \tag{11}$$

where

$$f_1 = f(u_1); \quad f_2 = f(u_2)$$

$$s^+_{1/2} = \max(0, a_1, a_2); \; s^-_{1/2} = \min(0, a_1, a_2)$$

To specify the scheme of eqs. (9)-(11), we have to define the values $u^l_{i+1/2}$ and $u^r_{i+1/2}$. When these values are defined as

$$u^l_{i+1/2} = u_i^{n+1}, \quad u^r_{i+1/2} = u_{i+1}^{n+1} \tag{12}$$

an implicit scheme is attained, which unconditionally satisfies the MND property, but shows too much diffusion.

On the other hand, if defined by

$$\begin{aligned} u^l_{i+1/2} &= u_i^n - 0.5(\lambda_i - 1)\delta u_i^n \\ u^r_{i+1/2} &= u_{i+1}^n - 0.5(\lambda_{i+1} + 1)\delta u_{i+1}^n \end{aligned} \tag{13}$$

it becomes a 2nd-order explicit scheme that meets the MND property under the following conditions:

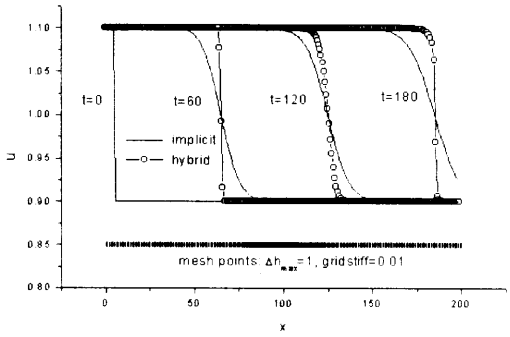

(a) Computed solutions; comparison between the hybrid and the fully implicit schemes

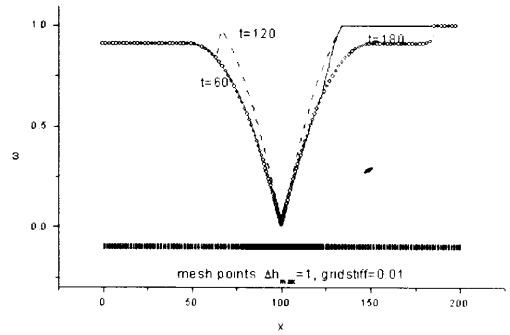

(b) Control parameter distributions

Figure 5: Case of a backward step-like initial distribution.

$$\beta_i^n \leq 1; \quad 0 \leq c^{\pm}_{i+1/2} \leq 2, \tag{14}$$

where

$$\beta_i^n = \frac{(s^{+,n}_{i-1/2} - s^{-,n}_{i+1/2})\Delta t}{\Delta x_i} \tag{14.1}$$

To make a the hybrid scheme, we propose cell interface values defined as follows:

$$u^l_{i+1/2} = u_i^n + (1 - \omega_i)\Delta^n u_i - 0.5(\omega_i \lambda_i - 1)\delta u_i^n \tag{15}$$

$$u^r_{i+1/2} = u_{i+1}^n + (1 - \omega_{i+1})\Delta^n u_{i+1} - 0.5(\omega_{i+1}\lambda_{i+1} + 1)\delta u_{i+1}^n \tag{16}$$

where $\Delta^n u$ denotes the time increment: $\Delta^n u = u^{n+1} - u^n$. As seen from these definitions, the interface values of the hybrid scheme are composed of two components. One corresponds to the implicit scheme of eq. (12), and the other to the explicit scheme of eq. (13). The parameter ω_i controls the amount of each component. It varies in the range

$$0 \leq \omega_i \leq 1 \tag{17}$$

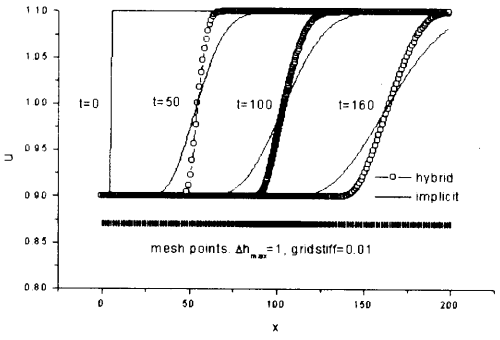

(a) Computed solutions; comparison between the hybrid and the fully implicit schemes

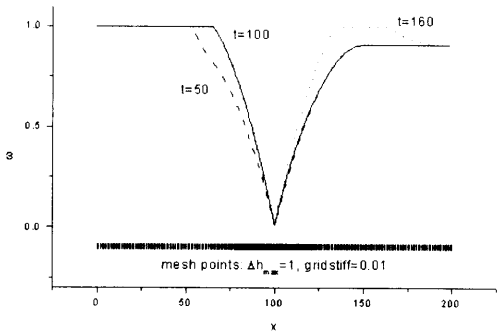

(b) Control parameter distributions

Figure 6: Case of a forward step-like initial distribution.

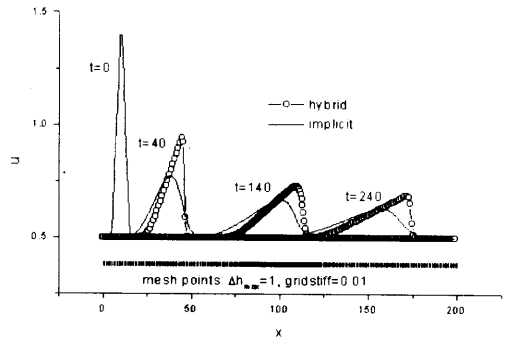

(a) Computed solutions; comparison between the hybrid and the fully implicit schemes.

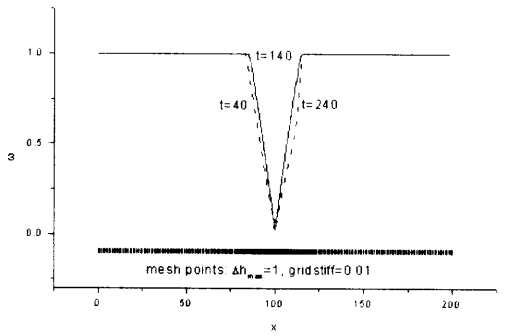

(b) Control parameter distributions

Figure 7: Case of a triangle-shape initial distribution.

When ω_i takes a value of zero or unity, the hybrid scheme becomes an implicit or an explicit scheme, respectively.

We can show a simple geometrical interpretation to the definition of edge states in the hybrid approach. To compute the values, first an intermediate time level: $t^{\omega_i} = t^n + \omega_i \Delta^n t$ is introduced for each cell (see Fig. 3), where intermediate values of the solution are defined by interpolating between the lower and upper time level values. Then, the explicit scheme is launched from the time level t^ω, using the intermediate values as initial data to obtain the edge states.

Evaluation of the control parameter is dictated by two conditions. To suppress strong diffusion inherent in the implicit scheme, it is preferable to take the value of this parameter as close to unity as possible, or even equal to unity. The other condition is that the scheme must keep the MND property. Therefore, an optimal decision is to take the value of ω as large as possible under the restriction that the scheme be max norm diminishing for all time steps. The lemma stated below helps us make such a decision.

LEMMA If the following inequalities are valid:

$$\omega_i \beta_i^\omega \leq 1, \quad 0 \leq c_{i+1/2}^{\pm} \leq 2 \tag{18}$$

the hybrid scheme (9),(10),(15),(16) hold the MND property.

In this lemma β_i is defined by eq. (14.1), and the superscript ω denotes the value evaluated at the time level t^ω. According to what has been stated by the lemma, we can define the control parameter as

$$\omega_i = \omega_*(\beta_i^\omega) \tag{19}$$

where the function ω_* is given by

$$\omega_*(x) = \begin{cases} 1 & x \leq 1 \\ \frac{1}{x} & x > 1 \end{cases}$$

Note that the hybrid scheme considered here exactly coincides with the CCG scheme for eq. (5), if eq. (19) for the evaluation of ω is replaced by $\omega_i = \omega_*(\beta_i^n)$.

2.2 Multidimensional Generalization

Multi-dimensional extension of the above hybrid scheme is carried out in a straightforward way. We consider a 3D equation in the form of the conservation law,

$$\partial_t u + \partial_k f_k(u) = 0, \quad (k = 1, ..., 3) \tag{20}$$

which is discretized by the FVM as

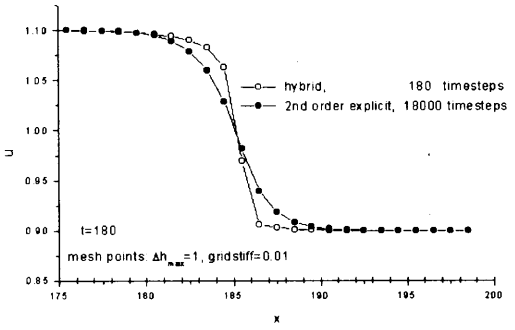

Figure 8: Comparison between the Hybrid and the Explicit Schemes for a backward step-like.

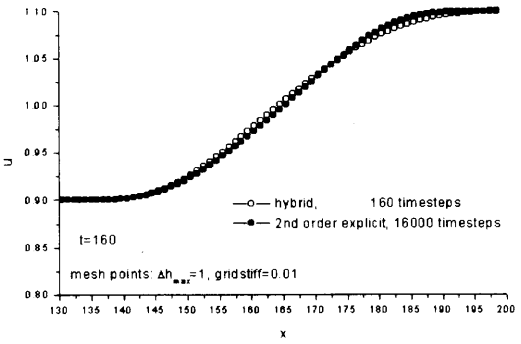

Figure 9: Comparison between the Hybrid and the Explicit Schemes for a forward step-like.

$$u_i^{n+1} = u_i^n - \frac{\Delta t}{\Delta V_i}\sum_\sigma F_\sigma \Delta \mathcal{S}_\sigma = 0 \qquad (21)$$

where ΔV_i denotes the cell volume, ΔS_σ the cell face area, and $F_\sigma = f_{k,\sigma}\, n_{k,\sigma}$ the numerical flux at the cell face. The summation is performed over all faces of the cell (see Fig. 4).

The numerical flux is approximated by a flux function of two arguments: face states on the left- and the right-hand sides

$$F_\sigma = f_{k,\sigma}\cdot n_{k,\sigma} = F(u_\sigma^l, u_\sigma^r) \qquad (22)$$

which is also calculated in the form of HLL approximation:

$$F(u_\sigma^l, u_\sigma^r) = \frac{s_\sigma^+ F_\sigma^l - s_\sigma^- F_\sigma^r + s_\sigma^+ s_\sigma^- (u_\sigma^l - u_\sigma^r)}{s_\sigma^+ - s_\sigma^-} \qquad (23)$$

where

$$F_\sigma^l = f_k(u_\sigma^l)\cdot n_{\sigma,k};\quad F_\sigma^r = f_k(u_\sigma^r)\cdot n_{\sigma,k}$$

$$s_\sigma^+ = \max(0, a_\sigma^l, a_\sigma^r);\ s_\sigma^- = \min(0, a_\sigma^l, a_\sigma^r)$$

Here $a = \vec{\alpha}\cdot\vec{n} = \alpha_k n_k$, and $\alpha_k = df_k/du$ $(k = 1,2,3)$.

Following the idea of hybridization developed above for 1D equations, let us write the left and right face states as:

$$\begin{aligned} u_\sigma^l &= u_i^n + (1-\omega_i)\Delta^n u_i + \left(\vec{r}_{i,\sigma} - 0.5\Delta t\omega_i\vec{\alpha}_i\right)\cdot\vec{\partial u}_i \\ u_\sigma^r &= u_{\sigma(i)}^n + (1-\omega_{\sigma(i)})\Delta^n u_{\sigma(i)} \\ &\quad + \left(\vec{r}_{\sigma(i),\sigma} - 0.5\Delta t\omega_{\sigma(i)}\vec{\alpha}_{\sigma(i)}\right)\cdot\vec{\partial u}_{\sigma(i)} \end{aligned} \qquad (24)$$

where $\vec{\partial u}_i$ is a limited gradient as

$$\vec{\partial u}_i\cdot\vec{r}_{i,\sigma} = c_i^\sigma \Delta u_{\sigma(i),i},\quad \Delta u_{\sigma(i),i} = u_{\sigma(i)} - u_i \qquad (25)$$

Here $0 \le c_i^\sigma \le +\infty$.

As seen here, the cell parameter ω_i again controls the amount of the explicit/implicit constituents in the hybrid scheme. Particularly, the scheme is fully implicit for $\omega_i = 0$ which is unconditionally of MND property.

As for $\omega_i = 1$, the scheme converts to a 2nd-order explicit scheme that possesses the MND property under the following conditions (see [3], also):

$$max\left(\beta_i^I, \beta_i^{II}\right) \le 1,\quad c_i^\sigma \le 0.5 \qquad (26)$$

for all cells and faces. β_i^I and β_i^{II} are calculated as

$$\begin{aligned} \beta_i^I &= \frac{1}{2}\Delta t\sum_\sigma b_i^\sigma\left(-\vec{\alpha}_i\right); \\ \beta_i^{II} &= \frac{\Delta t}{V_i}\sum_\sigma S_\sigma\gamma_\sigma^+\left[1 + \frac{1}{2}\sum_{\sigma'} b_i^{\sigma'}\left(\vec{z_i^\sigma}\right)\right] \end{aligned} \qquad (27)$$

In these formulas,

$$\gamma_\sigma^+ = \frac{s_\sigma^+\left[\left(\vec{\alpha}_i, \vec{n}_\sigma\right) - s_\sigma^-\right]}{s_\sigma^+ - s_\sigma^-} \qquad (28)$$

$$\vec{z_i^\sigma} = -\vec{r_i^\sigma} + 0.5\Delta t_i\vec{\alpha}_i$$

$b_i^\sigma\left(\vec{X}\right)$ denotes positive coefficients of a decomposition of a vector $\vec{X}$ with the face radius-vectors $\vec{r_i^\sigma}$:

$$\vec{X} = \sum_\sigma b_i^\sigma\left(\vec{X}\right)\vec{r_i^\sigma},\quad b_i^\sigma\left(\vec{X}\right) \ge 0$$

Such a decomposition always exists, if computational cells are convex.

Based on the MND conditions for the explicit scheme of eq. (26), the following lemma can be proved.

LEMMA If the control parameter ω_i satisfies the inequality

$$\omega_i\, max\left(\beta_i^{I,\omega}, \beta_i^{II,\omega}\right) \le 1 \qquad (29)$$

the hybrid scheme given by eqs. (21) - (25) is of MND property providing the limited gradient of eq. (25) is employed with $0 \le c_i^\sigma \le 0.5$ for all cells and faces.

Consequently from this lemma, we can define ω_i as

$$\omega_i = \omega_* \left(\beta_i^\omega\right), \quad \beta_i^\omega = max\left(\beta_i^{I,\omega}; \beta_i^{II,\omega}\right) \tag{30}$$

Note that the set of coefficients b_i^σ in eq. (27) is not unique. Some special algorithm to find such a set is required. Therefore, the calculation of β_i^ω in eq. (30) becomes expensive. To overcome this, a less restricted condition can be used[3], which leads to a more simple formula for β_i^ω:

$$\beta_i^\omega = \frac{\Delta t_i}{V_i} \sum_\sigma \mathcal{S}_\sigma \gamma_\sigma^+ \tag{31}$$

3 Solution of Discretized Equations

Except for the case $\omega_i = 1$, the discrete equations of the hybrid scheme have a complicated form. To find the upper time level solution u_i^{n+1} from these equations, we employ Newton's iteration method. With s as an iterative index, the linearization of eq. (21) can be written as

$$[\boldsymbol{I} + \boldsymbol{L}^s(\cdot)]\,\delta\Psi^s = \boldsymbol{R}^s - \Psi^s;$$

$$\Psi^s = u^{n+1,s} - u^n; \quad \delta\Psi^s = \Psi^{s+1} - \Psi^s \tag{32}$$

where

$$\boldsymbol{L}(\cdot) = \frac{\partial \boldsymbol{R}}{\partial \boldsymbol{U}} = \boldsymbol{D}(\cdot) + \boldsymbol{L}_1(\cdot) + \boldsymbol{L}_2(\cdot)$$

Here $\boldsymbol{R}$ denotes the residual on the right-hand side of eq.(21), and $\boldsymbol{D}$, $\boldsymbol{L}_1$, $\boldsymbol{L}_2$ are the diagonal, the lower- triangular, and the upper-triangular constituents of the matrix $\boldsymbol{L}$, respectively.

The solution to the linear system (32) is obtained by implementing sub-iterations with the LU-SGS method, where a couple of equations are successfully solved in the forward and backward iterative sweeps as follows:

$$[\boldsymbol{D} + \boldsymbol{L}_1(\cdot)]\,\delta\Psi^{s,*} + \boldsymbol{L}_2(\delta\Psi^{s,m}) = \boldsymbol{R}^s - \Psi^s$$

$$[\boldsymbol{D} + \boldsymbol{L}_2(\cdot)]\,\delta\Psi^{s,m+1} + \boldsymbol{L}_2(\delta\Psi^{s,*}) = \boldsymbol{R}^s - \Psi^s \tag{33}$$

Note that the exact linearization of eq. (32) is very expensive, if not impossible to obtain. In order to simplify the linearization, wave speeds $s_\sigma^\pm$ in the flux formula (23) and the control parameter ω as well are assumed to be "frozen". Moreover, only a first-order representation of the numerical fluxes, i.e. eqs. (27) and (24) with $\partial\vec{u}_i = 0$, is linearized.

4 Numerical Results

In this section, leaving aside theoretical aspects for a moment, we give some numerical results to show the effectiveness of the hybrid scheme. As a test case, we compute a one-dimensional Burgers equation:

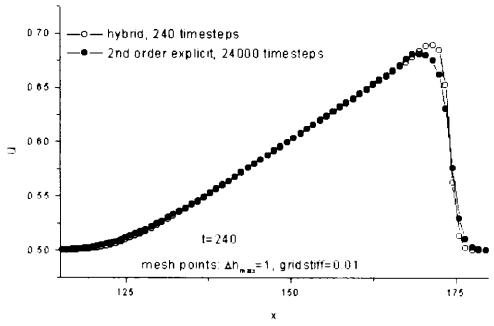

Figure 10: Comparison between the Hybrid and the Explicit schemes for a triangular initial data.

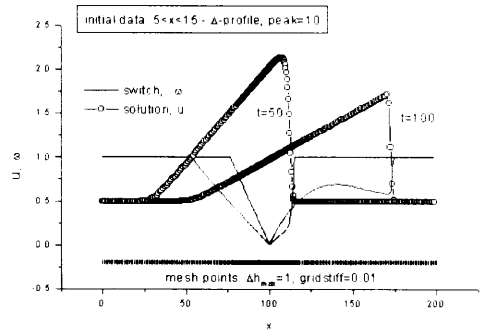

Figure 11: Hybrid scheme results for a high peak initial data.

$$\partial_t u + u\partial_x u = 0 \tag{34}$$

with several initial conditions.

These calculations used a computational grid with an interval $0 \leq X \leq 200$ and a grid stiffness ratio of 0.01. The maximal spacing is $\Delta h_{max} = 1$, while the minimal one is $\Delta h_{min} = 0.01$ which placed at $X = 100$, the center of the interval. The grid is also depicted in the figures.

Figures 5 to 7 show numerical results of computing eq. (34) with $\Delta t = 1$ for three initial data in the form of a backward step, a forward step, and a triangle. The results are obtained by the fully implicit scheme, $\omega_i = 0$, and the hybrid scheme. The dissipation of the fully implicit scheme is quite large, while the hybrid scheme well suppresses it. Distributions of ω in Figs. 5 to 7 show that it tends to unity as Δh increases, where the scheme mostly uses the explicit constituent rather than the implicit one. On the other hand, in the region where Δh is small, ω takes a small value, and the scheme switches to the implicit constituent.

Figures 8 to 10 show a comparison between the hybrid scheme and the 2nd-order explicit scheme. It is seen that the hybrid scheme maintains almost the same accuracy as the 2nd-order explicit scheme in spite of use of more than 100 times larger time step.

Figure 11 shows numerical solutions obtained by the hybrid scheme for a high-peak triangular initial data with a relatively large time step of $\Delta t = 1$.

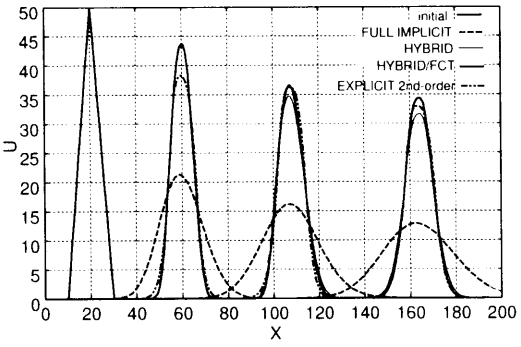

(a) Distributions of solution

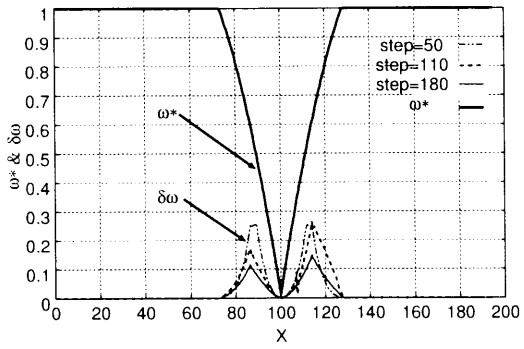

(b) Expansion Wave

Figure 12: Characteristics of Hybrid/FCT scheme.

"Expansion-type" and "shock-type" features of this solution are well captured, although the time step used in this calculation exceeds the CFL-allowable time step by several hundred times. Distributions of the switch parameter ω are also given, which show a rather complicated process of hybridization between the explicit and implicit constituents in the dense grid region.

5 Enforcement of Explicit Constituent

In the previous section, we confirmed the high performance of the baseline scheme. As mentioned in the introduction, to further develop the hybrid scheme, we can introduce a FCT technique to enforce the explicit constituent so as to keep the MND property. By doing this, we can get more accurate solutions for time dependent problems.

The FCT technique is introduced in the following way. Let us consider, for simplicity, a one-dimensional linear equation

$$\partial_t u + \partial_x f(u) = 0 \tag{35}$$

which is discretized by the hybrid scheme as

$$u_i^{n+1} = u_i^n - \frac{\Delta t}{\Delta x_i}\left[F_{i+1/2}(\omega_i^*) - F_{i-1/2}(\omega_i^*)\right] \tag{36}$$

Then, we introduce a new control parameter ω_i. It is determined by ω_i^* evaluated in the baseline scheme and $\delta\omega_i$ for an additional amount of the explicit constituent as

$$\omega_i = \omega_i^* + \delta\omega_i \tag{37}$$

Accordingly, the numerical flux function is transformed to

$$F_{i+1/2}(\omega_i) = F_{i+1/2}(\omega_i^*) + \delta F_{i+1/2} \tag{38}$$

where the additional flux $\delta F_{i+1/2}$ can be represented as

$$\delta F_{i+1/2} = A_{i+1/2}\delta\omega_i, \quad (0 \le \delta\omega_i \le 1 - \omega_*) \tag{39}$$

The coefficient $A_{i+1/2}$ can be treated as an anti-diffusion flux, which suppresses the dissipation. In this view, $\delta\omega_i$ in eq. (37) can be considered as an analogue of the limiting coefficient in the FCT method[4], and can be taken such that no new extremum would appear in the numerical solution. As a result of this procedure, the hybrid scheme might be more accurate. Figure 12 shows the effectiveness of this approach.

6 Concluding Remarks

A new hybrid implicit-explicit scheme has been developed for non-linear advection equations. The scheme holds the MND property for all time steps. The numerical results show its good performance and accuracy to solve time dependent problems with large time steps. Application of this scheme to compressible fluid dynamics equations is under way.

References

[1] Richtmyer, R. D. and Morton, K. W., "Difference methods for initial-value problems," Interscience Publishers, 1967.

[2] Collins, J., Collela, P., and Glaz, H.: "An Implicit-Explicit Eulerian Godunov Scheme for Compressible Flow," JCP, 116, pp. 195-211, 1995.

[3] O'Rourke, P. and Sahota, M., "A Variable Explicit/Implicit Numerical Method for Calculating Advection on Unstructured Meshes," JCP, 143, pp. 312-345, 1998.

[4] Zalesak, S., "Fully Multidimensional Flux-Corrected Transport Algorithms for Fluids," JCP, 31, pp. 335-362, 1979.

[5] Harten, A., Lax, P. D., Van Leer, B., "On Upstream Differencing and Godunov-Type Schemes for Hyperbolic Conservation Law," SIAM Review, 25, pp. 35-61, 1983.